Progress of Theoretical Physics, Vol. 87, No. 3, March 1992

Derivation of the 4-Body Bound-State Equation from the Effective Action

—— *Diagrammatical Legendre Transformation* ——

Ko OKUMURA

Department of Physics, Faculty of Science and Technology
Keio University, Yokohama 223

(Received October 30, 1991)

The 4-body bound-state equation is derived by use of on-shell expansion of the effective action. Derivation is based on the second derivative of the effective action which makes the graphical rule much easier. The essential tool is the sum-up rule of the graphs which is equivalent to the Legendre transformation. This rule can be widely used for any operator that has external point(s). Applied to the 1, 2, 3-body channels our method gives another way of deriving the known bound-state equations. The obtained equations hold whether the vacuum state is condensed or not.

§ 1. Introduction

The bound state problem in relativistic field theory has long been discussed starting from the bosonic Bethe-Salpeter (BS) equation for the 2-body bound state (Refs. 1)). Since then many authors discussed the solution and the formal properties of the bound-state equation (for example, see Refs. 2)). The 3-body bound-state equation has been obtained (Refs. 3), 4)) in the relativistic field theory. It will not be necessary to emphasize here the importance of generalizing BS equation for N-body channel. Indeed the Nth-order Bethe-Salpeter kernel was defined as a generalization of lower-order kernels (Ref. 5)) and its grahical properties have been studied by several authors (Refs. 6), 7)). But the derivation of the bound state equation for N-body channel is another subject.

N-body bound sate equation for general N has been recently obtained by use of the on-shell expansion of the effective action. However the arguments of Ref. 8) are limited to the case where the vacuum state is not a condensed one.

The purpose of this paper is to extend the on-shell expansion to derive 1, 2, 3 and 4-body bound-state equation in a way that they are valid whether the vacuum state is a non-perturbative one or not. By non-perturbative vacuum we mean the case that the true vacuum is a condensed state. A newly obtained result is the 4-body bound-state equation which can be used to determine the bound state excited above the condensed vacuum. (This will help us to understand what problem has to be solved in deriving the rules for the graphical expression of the N-body BS kernel ($N>4$) for the system whose vacuum is a condensed state.) The physical importance of the above problem is clear since we encounter the condensed vacuum in various systems; ferromagnet, superconductivity or quark-gluon system described by quantum chromodynamics (QCD).

In the on-shell expansion the bound-state equation is obtained by the second derivative of the effective action (Ref. 9)). Our result indeed reproduces the second derivative of effective action (up to the 4th one) obtained by De Dominicis and Martin (Ref. 10)). Their result has some exceptional graphs but ours does not contain them because they disappear when we take the second derivative. Their derivation of the 4th effective action has much combinatorial complexity. Several authors have tried to reduce the complexity and to make the proof simpler by using equations of motion for the Legendre transforms (Ref. 11)) or Spencer's t-derivative (Refs. 12), 6), 7)). Here instead we establish the *sum-up rule* which plays the central role in this paper. By the word *sum-up*, we mean that some small part of a larger graph is considered as generated by the corresponding full vertices and a class of graphs is summed up into a single simpler graph. For vacuum graphs, or for the effective action itself, sum-up rule does not hold, but for the second derivative of the effective action, the proof works since it is represented by the graphs with external lines. Recall that the second derivative is sufficient for the derivation of the bound-state equation. This rule also eliminates the complexity of the proof. The essential point is that the sum-up rule corresponds to the Legendre transformation required to define the effective action and leads to the concept of 4-particle-irreducibility of the graph.

Here we recall the definition of the effective action. The effective action Γ of field theory is given by the generating functional W of the Green's functions through the Legendre transformation (Ref. 13)). It is useful especially in the studies of spontaneous symmetry breaking (Ref. 14)). Moreover, it has been found that the effective action tells us all the physical quantities of a system considered quite systematically through the method of the on shell expansion; the stationary requirement to Γ determines the ground state, the lowest expansion of it around the stationary solution gives the bound-state equations, or the particle mode (Ref. 9)), and the higher order expansions correspond to the scattering amplitude among the particles (Refs. 15), 16)).

To exemplify the above method more specifically, we define $W[J]$, the generating functional for the Green's functions. Let us take a single component scalar field $\varphi(x)$ and introduce

$$\exp\left(\frac{i}{\hbar}W[J]\right)=\int[d\varphi]\exp\left(\frac{i}{\hbar}S_J\right), \tag{1·1}$$

$$\begin{aligned} S_J&=I[\varphi]+\sum_{j=1}^{N}\int d^4x_1\cdots\int d^4x_j\frac{1}{j!}J_j(x_1,\cdots,x_j)\varphi(x_1)\cdots\varphi(x_j) \\ &\equiv I[\varphi]+\sum_{j=1}^{N}\frac{1}{j!}J_j\,\varphi^j\,. \end{aligned} \tag{1·2}$$

The symbol $\int[d\varphi]$ stands for the path integration and $I[\varphi]$ is the classical action of the system considered. We have employed the symbolic notation by suppressing the space-time integration. This is used throughout the paper.

The i-th effective action, $\Gamma_i[\phi]$, is the i-fold Legendre transform of $W[J]$. Let us define the i-body Green's function ϕ_i and Γ_i,

$$\phi_i(x_1,x_2,\cdots,x_i)=-i!\frac{\delta W[J]}{\delta J_i(x_1,x_2,\cdots,x_i)}\equiv -i!\frac{\delta W[J]}{\delta J_i}\,, \tag{1·3}$$

$$\Gamma_i = W + \sum_{j=1}^{i} \frac{1}{j!} J_j \phi_j \,. \tag{1·4}$$

Then the following equations are easily verified:

$$J_i = i! \frac{\delta \Gamma_j}{\delta \phi_i} \,, \quad (i \leq j) \tag{1·5}$$

$$\phi_i = -i! \frac{\delta \Gamma_j}{\delta J_i} = -i! \frac{\delta W}{\delta J_i} \,. \quad (i > j) \tag{1·6}$$

Note in the above formulae that the space-time variables are included in the indices (i and j). Note also that Γ_i's are functionals of ϕ_j and J_k where $j \leq i$ and $k > i$, that is, $\Gamma_i = \Gamma_i[\phi_1, \cdots, \phi_i, J_{i+1}, \cdots, J_N]$. The stationary solution $\phi_i^{(0)}$ to $\delta\Gamma/\delta\phi_i = 0$ determines the vacuum and zero eigenvalue equation (Ref. 9))

$$\sum_j \left(\frac{\delta^2 \Gamma_N}{\delta \phi_i \delta \phi_j} \right)_0 \Delta\phi_j = 0 \tag{1·7}$$

or equivalently, as is proved in Appendix A,

$$\left(\frac{\delta^2 \Gamma_N}{\delta \phi_N \delta \phi_N} \right)_0 \Delta\phi_N = 0 \tag{1·8}$$

is nothing but the mode-determining equation in the N-body channel, i.e., N-body BS equation in our case. Here $\sum_j$ implies the integral $\prod_{i=1}^{N} \int d^4 x_i$ and $(\cdots)_0$ signifies that it is evaluated at the solution $\phi_i^{(0)}$ which can be either the perturbative or the non-perturbative condensed vacuum.

In case the ground state is a perturbative one, $\phi_i^{(0)}$ can be expanded in the coupling constant so that the diagrammatical expansion of the kernel $(\delta^2\Gamma/\delta\phi_N\delta\phi_N)_0$ is available. If, on the other hand, the theory realizes the non-perturbative vacuum, $\phi_i^{(0)}$ has no perturbative expansion in the coupling constant but the rule for $(\delta^2\Gamma/\delta\phi_N\delta\phi_N)_0$ can be obtained in our case since the full vertices ϕ_i are our independent variables.

In § 2, the model is specified for simplicity but the arguments below can be easily generalized to any models. The 4-body BS equation is derived in § 3 carrying out the 4-fold Legendre transformation step by step by using the sum-up rule. The 1, 2, and 3-BS equations are also derived as a check in § 4 making use of the results of § 3. Appendix A contains the derivation of the formal N-body BS equation from effective action. In Appendix B some of the details of the sum-up rule are given, and in Appendix C an interesting relationship between two classes of graphs is presented which is utilized in § 3.

§ 2. Specification

For simplicity*) we will discuss the model described by the action

*) All the derivation below will be carried out for the bosonic field but the generalization to other fields including fermions is straightforward if we use the Grassmann algebra.

$$S_J=-\frac{1}{2}\int d^4x\int d^4y\varphi(x)(\Box+m^2)\varphi(y)$$
$$+\sum_{j=1}^{N}\int d^4x_1\cdots\int d^4x_j\frac{1}{j!}J_j(x_1,\cdots,x_j)\varphi(x_1)\cdots\varphi(x_j)$$
$$\equiv J_1\varphi-\frac{1}{2}\varphi(\Box+m^2-J_2)\varphi+\sum_{j=3}^{N}\frac{1}{j!}J_j\varphi^j\,. \tag{2·1}$$

Interactions will be taken into account by setting artificially introduced external source J equal to λ, the physical coupling constant, after all calculations. So, in the case of $\lambda\varphi^4$-theory, for example, we set

$$J_i=i!\frac{\delta\Gamma_N}{\delta\phi_i}=\lambda\delta_{i,4} \tag{2·2}$$

to determine $\phi_i^{(0)}$ or the ground state. The equation for determining the value of $\phi_i^{(0)}$ is already known,*) so we can formally proceed to get BS equation based on this solution $\phi_i^{(0)}$.

Because $W[J]$ is a class of all connected vacuum graphs built with vertex $J_k(k=1,2,\cdots,N)$ vertices and bare propagators, $\phi_2{}^0=\frac{\hbar}{i}(\Box+m^2-J_2)^{-1}$, ϕ_i is a class of all graphs with i external lines. Note here that $W[J]$ is *not* the generating functional for *connected* Green's functions. The connected i-body Green's functions $\phi_i{}^c$ are defined as a class of all possible connected graphs that appear as an element of ϕ_i. There is clearly a relation,

$$\phi_i=\phi_i{}^c+\text{polynomial of }\phi_j{}^c\quad\text{where } j<i\,.\quad(\text{especially }\phi_1=\phi_1{}^c) \tag{2·3}$$

Here polynomial of $\phi_j{}^c$ represents the disconnected parts. We can therefore regard Γ_i as a functional of $\phi_j{}^c$ and J_k where $j\leq i$ and $k>i$, that is, $\Gamma_i=\Gamma_i^c[\phi_1{}^c,\cdots,\phi_i{}^c,J_{i+1},\cdots,J_N]$.

Using Eq. (2·3), we can verify

$$\frac{\delta\Gamma_N{}^c}{\delta\phi_N{}^c}=\frac{\delta\Gamma_N}{\delta\phi_N}=\frac{1}{N!}J_N\,, \tag{2·4}$$

$$\frac{\delta^2\Gamma_N{}^c}{\delta\phi_N{}^c\delta\phi_N{}^c}=\frac{\delta^2\Gamma_N}{\delta\phi_N\delta\phi_N}\,. \tag{2·5}$$

In each line the first(second) expression implies that the derivative is taken regarding $\phi_j{}^c(\phi_j)(j=1,2,\cdots,N-1)$ as constant. Keeping Eq. (2·4) in mind, it is easy to see that

$$\left.\frac{\delta\phi_N{}^c}{\delta J_N}\right|_{\phi_1{}^c,\cdots,\phi_{N-1}^c}=\left[N!\frac{\delta^2\Gamma_N{}^c}{\phi_N{}^c\phi_N{}^c}\right]^{-1}, \tag{2·6}$$

where on the left-hand side the derivative is taken for fixed $\phi_j{}^c(j=1,2,\cdots,N-1)$ and on the right-hand side we regard $\phi_j{}^c(j=1,2,\cdots,N-1)$ as constant. Recall here that the right-hand side of Eq. (2·6) is written in terms of $\phi_1{}^c,\phi_2{}^c,\cdots,\phi_N{}^c$. Equation (2·6) enables us to study the second derivative of effective action by examining the graphi-

*) The graphical expression for $\delta\Gamma_i/\delta\phi_i$ or $J_j(j\leq4)$ in terms of ϕ-vertex is given in Ref. 10).

cal rule of the first derivative of connected Green's function with respect to J_N.

§ 3. 4-body BS equation

We first discuss the second derivative of the 4th effective action ($N=4$)*) by examining $\phi_4{}^c$. The reason why $\phi_4{}^c$ is taken is that we are interested in the 4-body BS equation. But the argument given in the following can be applied to any operator other than $\phi_4{}^c$ if the operator has external point(s). The result is given in Eq. (3·12) below. After this has been done it is easy to apply the arguments to $N=1, 2, 3$, which will be given in § 4.

For this purpose we have to derive graphical expressions of $\delta\phi_4{}^c/\delta J_4$ built with $\phi_1{}^c$, $\phi_3{}^c$, $\phi_4{}^c$-vertices and $\phi_2{}^c$-propagators. If this is done we get what we want through Eq. (2·6) for $N=4$. Of course, $\phi_4{}^c$ is originally given by the graphical expression written in terms of $J_1, \cdots, J_4$-vertices and bare propagators, so we have to eliminate J_i in favor of $\phi_i{}^c$ in the graphical terms. These operations correspond to the Legendre transformations given by Eq. (1·4); inverting Eq. (1·3) in favor of ϕ_i to get Eq. (1·5).

In the following subsections these procedures of replacement are performed successively starting from the transformation from J_1 to $\phi_1{}^c$. In each step we sum up a certain class of graphs and regard them as a single graph. The essential point in this process is that we have to clarify what criteria can be used to keep correct weight**) of each graph.

3.1. *The transformation from J_1 to $\phi_1{}^c$*

Let us start from a transformation from J_1 to $\phi_1{}^c$ by an appropriate process of summation. Although what we discuss in this subsection may be a well-known fact, we reproduce it here in our terminology because it will play an important role in the general arguments below. In the first place we consider a class of graphs contained in $\phi_4{}^c$ shown on the left-hand side of Eq. (3·1). Here black dots stand for J_i vertices.

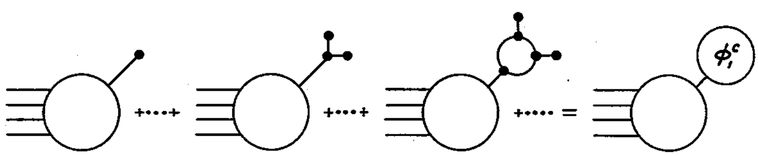

(3·1)

Here the lines in any graph denote the bare propagators. These graphs seem to be summed up to the right-hand side, but does each graph appear with correct weight?

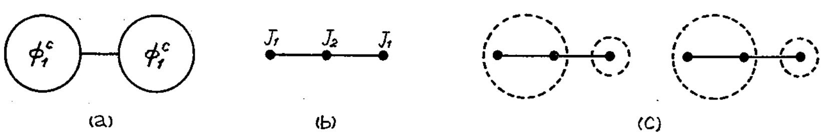

Fig. 1. The example of troublesome graph.

*) If the theory contains interaction such as $\lambda\varphi^6$, S_J should also include it, but the proof below does not change.

**) We use the correct (or right) weight of the graph in the sense that we get such weight if we regard the corresponding graph as the one appearing in the Green's function.

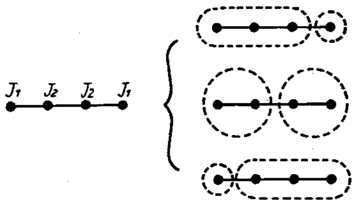

Fig. 2. Another example of troublesome graph.

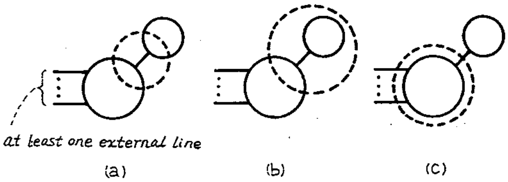

Fig. 3. Explanation of the larger 1-legged part.

In the above case the answer is definitely yes. Consider, however, the case described in Fig. 1. Of course, Fig. 1(a) contains the graph of (b). It is, however, not known that to which $\phi_1{}^c$ the J_2 vertex at the center of (b) should belong (see (c)). The same ambiguity occurs in all graphs contained in Fig. 1 (a) as shown in Fig. 2. In such cases it seems impossible to sum up a set of graphs into one simpler graph with right weight. The origin of such difficulty is of course that the graph has no external lines. Indeed, the diagrams appearing in Eq. (3·1) do not cause such difficulties. To show this we define a 1-*legged part* which is a connected subgraph in the elements of $\phi_4{}^c$ jointed to the rest through only one line (bare propagator). This is denoted by a closed (broken) line which encircles the subgraph and intersects only one line. In what follows we draw *a closed (broken) line so that it intersects one line (directly connecting one vertex or external point and another vertex) only once at most.* We also define a *larger 1-legged part* as a 1-legged part consisting of more vertices. The problem is whether we can unambiguously proceed to encompass a larger 1-legged part. This problem becomes important when two 1-legged parts have a common part; Case (a) — the two 1-legged parts inevitably intersect with each other or Case (b) — one completely contains the other. In Case (a) we cannot determine without ambiguity to which 1-legged part that common part belongs. But as is shown below two 1-legged parts can have a common part only when one completely contains the other one, *except the graphs with no external line* as described symbolically in Fig. 1(a). This is understood if we consider the case described in Fig. 3. We notice that we cannot draw broken lines like Figs. 3(a), (c), because a closed broken line intersects only one line and the graph is a connected one (these constraints inevitably contradict with each other). Thus the only possible broken line is shown in Fig. 3(b) in which it completely contains the other 1-legged part. This means that we can unambiguously reach a *largest 1-legged part* in any graphs of $\phi_4{}^c$. It is thus possible to proceed to a largest 1-legged part starting from any 1-legged part contained in a given graph. We continue this procedure until there are no 1-legged parts other than the largest ones (there may be many non-overlapping largest parts in a given graph). This is done for all the graphs of $\phi_4{}^c$. Two graphs are said to belong to *the same element of* $\phi_4{}^c$ if the two graphs have the same largest 1-legged structure (recall that graphs contained in each largest 1-legged part are different from one another). Then we put together all the graphs belonging to the same element of $\phi_4{}^c$. It is easy to see that this class of graphs corresponds with right weight to only one graph which is obtained by replacing all the largest 1-legged parts with the $\phi_1{}^c$'s. Through the above procedure we finally accomplish the transformation from J_1 to $\phi_1{}^c$. The result is

$\phi_4{}^c[\phi_1{}^c, J_2, J_3, J_4]=$ 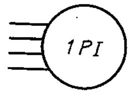 , (3·2)

where *1PI* (1-particle irreducible) implies that if the 4 external lines are connected by a J_4 vertex then the subsequent vacuum graph is 1PI.

Here we have used the following definition of 1PI (or iPI in general where $i=1$, 2, 3). A given connected vacuum graph is called 1PI (iPI) if it is separated into two parts only when at least $2(i+1)$ lines are cut except for the case that one of the separated parts is a trivial $\phi_1{}^c(\phi_2{}^c, \cdots,$ or $\phi_i{}^c)$-vertex.

3.2. *The transformation from J_2 to $\phi_2{}^c$*

Next the transformation from J_2 to $\phi_2{}^c$ is considered. Here we assume that $\phi_4{}^c$ is a functional of $\phi_1{}^c$, J_2, J_3 and J_4. Notice that it is already a functional of $\phi_1{}^c$.

Consider a graph of $\phi_4{}^c[\phi_1{}^c, J_2, J_3, J_4]$ having the structure of Fig. 4. Here B-part is a *2-legged part* which is a connected subgraph of $\phi_4{}^c[\phi_1{}^c, J_2, J_3, J_4]$. It is connected to the rest by two lines (bare propagators). The 2-legged part is indicated by a closed (broken) line intersecting two lines.

As in the previous subsection, we prove below that we can proceed without ambiguity to encompass a *larger-2-legged part*, that is, when two 2-legged parts have a common part with each other, one contains the other or otherwise there is another larger 2-legged part that completely contains these two 2-legged parts. If it is true, the largest 2-legged part is well-defined and all the graphs of $\phi_4{}^c[\phi_1{}^c, J_2, J_3, J_4]$ can be made to have no 2-legged parts other than the largest 2-legged parts. Two graphs are defined to be *the same elements of* $\phi_4{}^c[\phi_1{}^c, J_2, J_3, J_4]$ if both have the same largest 2-legged structure. Then we put together all the graphs belonging to the same element of $\phi_4{}^c[\phi_1{}^c, J_2, J_3, J_4]$. This class of graphs corresponds with right weight to a single graph which is obtained by replacing all the largest 2-legged parts with the $\phi_2{}^c$'s. Through the above procedure we finally accomplish the transformation from J_2 to $\phi_2{}^c$. Employing the notation where the line in the graph represents $\phi_2{}^c$, we have

$\phi_4{}^c[\phi_1{}^c, \phi_2{}^c, J_3, J_4]=$ 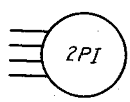 . (3·3)

Here 2PI implies that if the 4 external lines are connected by a J_4 vertex, then the resulting vacuum graph is 2PI.

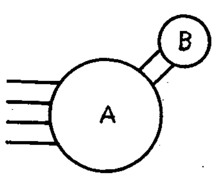

Fig. 4. A graph of $\phi_4{}^c[\phi_1{}^c, \phi_2{}^c, J_3, J_4]$.

Now we go back to Fig. 4 to prove the above statement. Suppose there exists a 2-legged part which *partially* contains B-part. Such cases are shown in Fig. 5. The *partially* excludes the case like Fig. 6 because the 2-legged part denoted by the broken line completely contains B-part. Taking into account the fact that each closed broken line

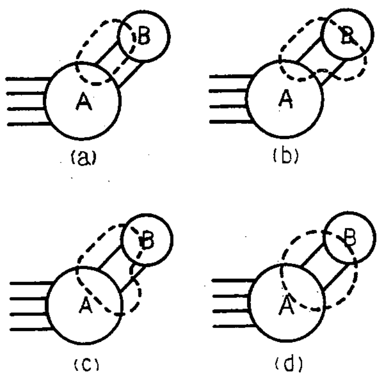

Fig. 5. The 2-legged parts partially containing B-part.

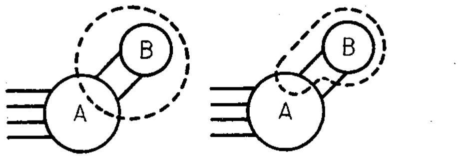

Fig. 6. The 2-legged parts completely containing B-part.

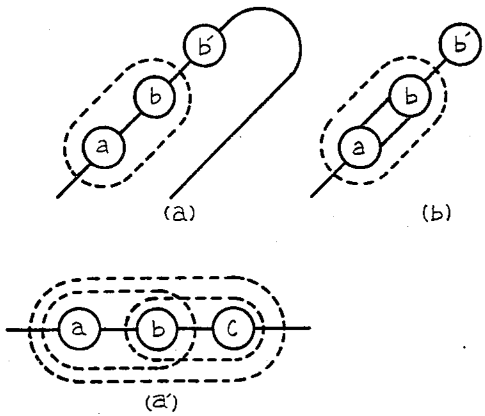

Fig. 7. More detailed structure of Fig. 5: The a- or b-(b′-) part corresponds to subparts of A- or B-part respectively.

can intersect just 2 lines, and that the graphs are connected ones, the cases shown in Figs. 5(b), (c) cannot occur. The graphs of Figs. 5(a), (d) have the following structures (Fig. 7). We notice that the case in Fig. 7(d) does not exist from the beginning because we are dealing with *1PI graphs* which are already functional of ϕ_1^c. In the case of Fig. 7(a) there are three ways to encompass 2-legged parts as shown in Fig. 7(a′) but there is the largest 2-legged part which completely includes the others.

The graphs in Fig. 5 do not include the cases in which the broken line intersects the external lines. But we notice that the case of Fig. 5 and the corresponding Fig. 7 include that of Fig. 8 and that we need not consider the case where the closed broken

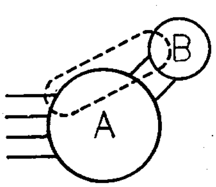

Fig. 8. The 2-legged part intersecting an external line.

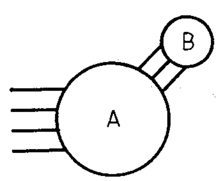

Fig. 9. A graph of $\phi_4{}^c[\phi_1{}^c, \phi_2{}^c, J_3, J_4]$.

line intersects more than two external lines because the closed broken line can intersect just two lines. Since A-part has external lines, we have exhausted all possible cases, so the statement has been proved.

3.3. *The transformation from J_3 to ϕ_3^c*

In this subsection we make a transformation from J_3 to ϕ_3^c by considering $\phi_4^c[\phi_1^c, \phi_2^c, J_3, J_4]$ which is already a functional of ϕ_1^c(vertex) and ϕ_2^c (line).

Let us consider one of the graphs of $\phi_4^c[\phi_1^c, \phi_2^c, J_3, J_4]$ which has the structure shown in Fig. 9. Note that all the lines in the graph stand for the ϕ_2^c's. As in the previous subsections we consider another 3-*legged part* which partially contains both A- and B-parts. We can prove the following statement in this case (see Appendix B); that is, we can unambiguously proceed to encompass a *larger* 3-*legged part,* namely, when two 3-legged parts have a common part with each other, one completely contains the other, otherwise there is another larger 3-legged part that completely contains these two 3-legged parts.

We thus arrive at the following result in the same way as in the previous subsections,

$$\phi_4^c[\phi_1^c, \phi_2^c, \phi_3^c, J_4]= \qquad (3\cdot4)$$

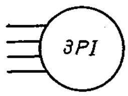

Here what is implied by *3PI* may be clear.

Now we can differentiate Eq. (3·4) by J_4 fixing ϕ_1^c, ϕ_2^c and ϕ_3^c. This gives

$$4!\frac{\delta\phi_4^c(a)}{\delta J_4(b)}\bigg|_{\phi_1^c, \phi_2^c, \phi_3^c}= \qquad (3\cdot5)$$

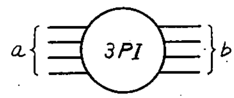

The above *3PI* implies that when two sets ((a) and (b)) of 4 external lines are closed by $J_4(a)$ and $J_4(b)$ vertices, the resulting vacuum graph is 3PI. The factor 4! on the left-hand side appears for the purpose of keeping the correct weight.

The cases in which right (a) and left (b) sets of 4 external lines are connected by less than 4 lines (Fig. 10) are excluded because the above derivative is taken by fixing ϕ_1^c, ϕ_2^c and ϕ_3^c.

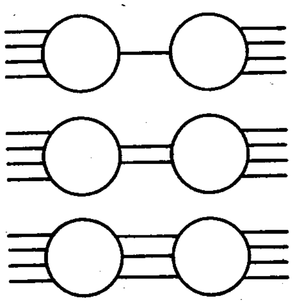

Fig. 10. The graphs excluded in Eq. (3·5).

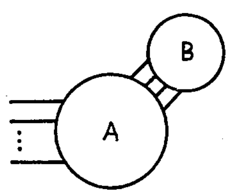

Fig. 11. A graph of $\delta\phi_4^c[\phi_1^c, \phi_2^c, \phi_3^c, J_4]/\delta J_4$.

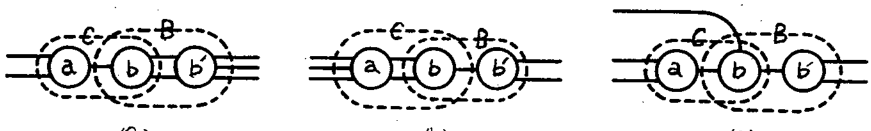

(a) (b) (c)

Fig. 12. The examples of troublesome structures.

3.4. *The transformation from J_4 to ϕ_4^c*

Consider the final transformation from J_4 to ϕ_4^c and express $\delta\phi_4^c/\delta J_4$(Eq. (3·5)) as a functional of ϕ_4^c. Note that ϕ_4^c is a functional of ϕ_1^c, ϕ_2^c and ϕ_3^c at this point.

We consider one of the graphs of $\delta\phi_4^c/\delta J_4$ which has the structure given in Fig. 11. Imagine, as in the previous subsections, another 4-*legged part* which partially contains both A- and B- parts. Here we encounter a difficulty; there arises an ambiguity in defining the *larger* 4-legged part. This is a crucial difference compared with the previous subsections. Indeed, the structures shown in Fig. 12 bring about a serious problem. The two 4-legged parts (B, C) have a common part, but there is not the third 4-legged part which completely contains B- and C-parts. For the detailed discussions on the structure of these graphs, see Appendix B. We realize from these examples that if the graph contains the substructure shown in Fig. 13 (this type is called the *pseudo 4-vertex*), a *largest 4-legged part* loses its meaning. So we introduce another variable $\phi_4^{c,p}$ and try to make a transformation from J_4 not to ϕ_4^c but to $\phi_4^{c,p}$,

$$\phi_4^{c,p}(1,2,3,4)\equiv\phi_4^c(1,2,3,4)-$$

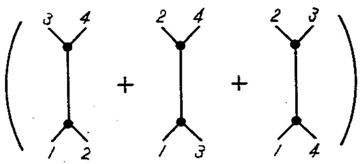

, (3·6)

where the black dot stands for ϕ_3^c. The pseudo 4-vertices are thus excluded from the definition of 4-legged parts. Then in Figs. 12(a), (b) there is only one way to draw a closed broken line as 4-legged part, i.e., the lines B, C respectively in the figures, and no way in Fig. 12(c). The *largest 4-legged part* can now be defined, and the transformation from J_4 to $\phi_4^{c,p}$ is accomplished. After the transformation, we get

$$4!\frac{\delta\phi_4^c(a)}{\delta J_4(b)}\bigg|_{\phi_1^c,\phi_2^c,\phi_3^c}=$$

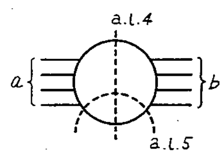

. (3·7)

On the right-hand side *a.l.4* (at least 4) and *a.l.5* mean that the graphs meet the following constraints. Suppose that 4 external lines on both sides of a graph of Eq. (3·7) be connected by two extra $\phi_4^{c,p}(a)$, $\phi_4^{c,p}(b)$ to make a vacuum graph. If the resulting vacuum graph is separated into two parts in such a way that no line connects $\phi_4^{c,p}(a)$ with $\phi_4^{c,p}(b)$, then at least 4 lines have to be cut. Otherwise, at least 5 lines must be cut in order to separate it except for the case where one of the separat-

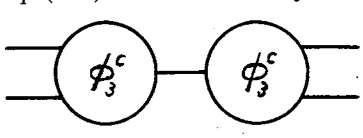

Fig. 13. The pseudo 4-vertex.

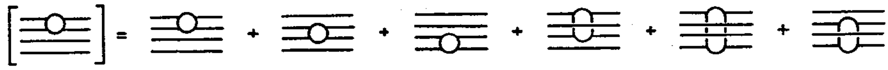

Fig. 14. The generator of the simple net: The circle stands for $\phi_4^{c,p}$ (or pseudo 4-vertex).

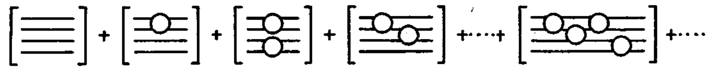

Fig. 15. The simple net: We include the first term for convenience.

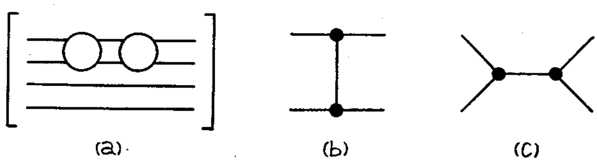

Fig. 16. Explanation of simple net: The circle in (a) and black dots in (b) and (c) stand for ϕ_4^c(or pseudo 4-vertex) and ϕ_3^c respectively.

ed parts is a trivial ϕ_1^c, ϕ_3^c or $\phi_4^{c,p}$ (or pseudo 4-vertex).

Let us study the graph shown in Fig. 14. In what follows, the square bracket [⋯] implies the sum of the permutation of the external lines on the left- and right-hand side of the graph. In this definition the permutation of one external line on the right-hand side with the one on the left-hand side is not allowed. Consider a particular set of graphs obtained by the iteration of Fig. 14 and included on the right-hand side of Eq. (3·7) as well. This particular class of the graphs generated by 6 different elements in Fig. 14 which meets a.l.4 and 5 conditions of Eq. (3·7) is called *simple net* and is shown in Fig. 15. This set does not contain such parts as Fig. 16(a) because it is inconsistent with the fact that we have already taken the largest 4-legged parts in Eq. (3·7) by using $\phi_4^{c,p}$. The pseudo 4-vertex can appear in 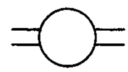 only in a way of Fig. 16(b) because if it is contained in the graph in a way of Fig. 16(c) this part contradicts with a.l.4 condition of Eq. (3·7). It is easily understood that the simple net composed of combination of $\phi_4^{c,p}$ and pseudo 4-vertices can be written by a simple net built only with D_4 defined as

$$D_4(1,2;3,4)\equiv\phi_4^{c,p}(1,2,3,4)+ \tag{3·8}$$

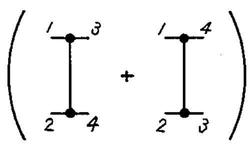

Note that D_4 should be used in a way that is consistent with a.l.4 condition of Eq. (3·7). We call this simple net D_4 *simple net*. Noticing that the graphs appeared in Eq. (3·7) are able to be classified by the number of D_4 simple net where we can make the graph apart by cutting 4 lines, the following relation is readily written down,

$$\left.\frac{\delta\phi_4^c}{\delta J_4}\right|_{\phi_1^c,\phi_2^c,\phi_3^c}=$$

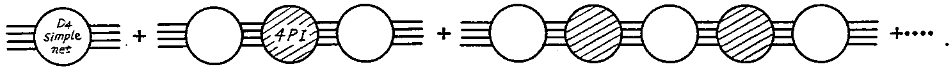

(3·9)

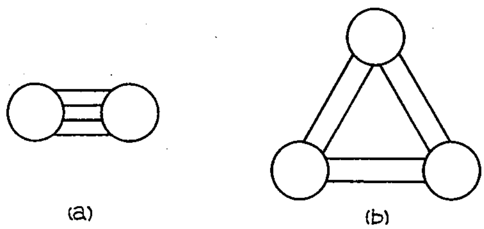

Fig. 17. The explanation of 4PI: The circle stands for $\phi_4^{c,p}$ (or pseudo 4-vertex).

Here 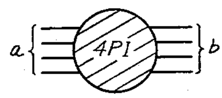 means the class of graphs which satisfies the following condition.*) Suppose that 4 external lines on both sides of the graph be connected by two extra $\phi_4^{c,p}(a)$, $\phi_4^{c,p}(b)$ to get a vacuum graph. If this vacuum graph is separated into two parts, at least 5 lines must be cut except for the case that one of the separated parts is a trivial ϕ_1^c, ϕ_3^c or $\phi_4^{c,p}$ (or pseudo 4-vertex). Note that another constraint should be added to the definition of 4PI to eliminate the first two terms of the D_4 simple net from the 4PI graph; the resulting vacuum graph does not correspond to Fig. 17. Strictly speaking, in order to keep the right weight of the graph, we should associate the factor 1/4! with every D_4 simple net and 4PI part in Eq. (3·9). This point will be mentioned in § 4.

Let us use here the following very interesting theorem which is proven in Appendix C.

THEOREM 1 *D_4 simple net* $=[$*D_4 chain*$]^{-1}$,

where D_4 chain means the class of graphs given in Fig. 18. It is a class of the graphs created by the second derivative by D_4 of the sum of the cyclic vacuum graphs shown in Fig. 19. Thus we obtain

$$\left.\frac{\delta\phi_4^c}{\delta J_4}\right|_{\phi_1^c,\phi_2^c,\phi_3^c}=$$ 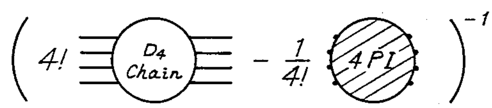

(3·10)

Then we reach the final result for the BS kernel.

$$\frac{\delta^2\Gamma_4^c}{\delta\phi_4^c\delta\phi_4^c}=$$ 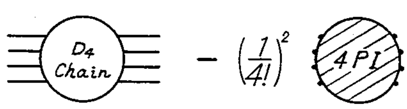

(3·11)

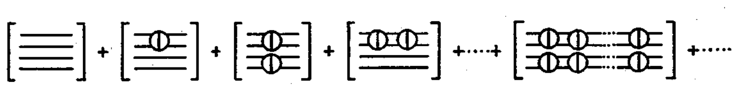

Fig. 18. The chain: 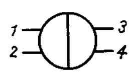

stands for $D_4(1, 2; 3, 4)$ in what follows.

*) This is also expressed in terms of *cycle of pairs* defined in Ref 10).

This result corresponds with the second derivative of the main result in Ref. 10). Therefore, the following equation,

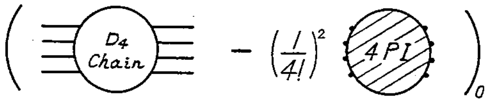

$$\Delta\phi_4{}^c=0 \qquad (3\cdot12)$$

is our generalized 4-body BS equation. In Eq. (3·12) the integration over space-time coordinate is suppressed and $[\cdots]_0$ implies that $[\cdots]$ is evaluated at the solution $\phi^{(0)}$ to $\delta\Gamma/\delta\phi=0$. Equation (3·12) is the main result of this paper.

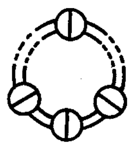

Fig. 19. The cyclic vacuum graph.

§ 4. 1, 2, 3-body equations

In this section we give the second derivative of the 1st, 2nd and 3rd effective actions by our method presented in the previous section. It will be seen that they coincide with those in Ref 10). Since we have already worked out the 4th effective action, this is straightforward. By this process we can check the validity of our sum-up rule but on the other hand it sheds light on the problems which occur in the case of effective action of higher order than the 4th. We come to this point at the end of this section.

We start with the 1st effective action. We notice that J_1 vertex in $\delta\phi_1{}^c/\delta J_1$ can be replaced by $\phi_1{}^c$ as in § 3.1 and get

$$\left.\frac{\delta\phi_1{}^c}{\delta J_1}\right|_{J_2,J_3,J_4}= \qquad (4\cdot1)$$

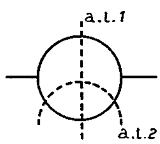

The definition of $a.l.i$ and $a.l.i+1$ $(i=1,2,3)$ can be given analogously with the previous sections, that is, "The vacuum graph is first defined by attaching two $\phi_i{}^c$'s on both sides of the graph. This can then be separated into two parts only when at least i or $i+1$ lines are cut depending on whether the two attached $\phi_i{}^c$'s remain connected or not, except for the case that one of the separated parts is a trivial vertex $\phi_k{}^c$ $(1\leq k\leq i)$." Note that for the first effective action $(i=1)$ the lines are bare propagators.

We can classify the graphs of the right-hand side of Eq. (4·1) by the number of lines which lead two separate graphs if one of them is cut,

$$\left.\frac{\delta\phi_1{}^c}{\delta J_1}\right|_{J_2,J_3,J_4}= \qquad (4\cdot2)$$

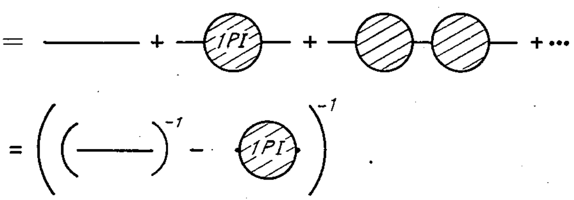

Here 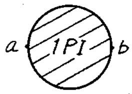 is usually called the self-energy part and *1PI* implies that if each external point a, b is closed by a $\phi_2{}^0 J_4$ (vertex with bare propagator) then the subsequent vacuum graph is 1PI. So using Eq. (2·6), we get the BS-kernel and the BS equation for 1-body case,

$$\frac{\delta^2 \Gamma_1{}^c}{\delta\phi_1{}^c \delta\phi_1{}^c}=$$ 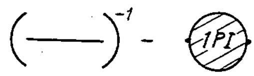 , (4·3)

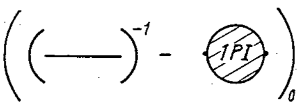 $\Delta\phi_1{}^c=0$ (4·4)

which determine the energy of the one-particle state and $\Delta\phi_1{}^c$ is nothing but 1-body wave function.

In order to study the 2-body case we notice that J_1 vertex in $\phi_2{}^c$ can be replaced by $\phi_1{}^c$ vertex as in § 3.1 and get

$$\phi_2{}^c=$$ 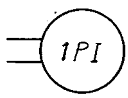 , (4·5)

where 1PI means that the vacuum graph obtained by supplying two J_2 vertices is 1PI. Then replacing J_2 with $\phi_2{}^c$, we get

$$2!\frac{\delta\phi_2{}^c}{\delta J_2}\bigg|_{\phi_1{}^c, J_3, J_4}=$$ 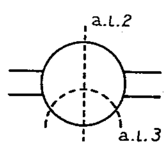 . (4·6)

The meaning of *a.l.2* and *3* has already been defined. Note that lines here are the $\phi_2{}^c$'s. Then we notice that

$$\frac{\delta\phi_2{}^c}{\delta J_2}\bigg|_{\phi_1{}^c, J_3, J_4}=$$ 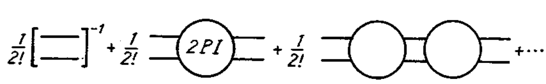 . (4·7)

Consider the weight of the graphical expression on the right-hand side. Suppose that one of the graphs of the third term contains $p+q$ vertices and that the left 2PI part contains p vertices and the right q vertices. For simplicity we assume that this graph contains only one kind of vertex. We can obtain the weight of this graph by the following steps.

1. Distribute $p+q$ vertices to the two 2PI parts ($C(p, q)\equiv(p+q)!/(p!q!)$ ways).
2. Calculate the weight for each 2PI part separately by considering the lines connecting two 2PI parts as fixed external points.

3. Connect the two 2PI parts with the factor $1/2!$.

Note that these steps can be applied regardless of whether 2PI parts are symmetric graphs or not with respect to the above artificial external points. Note also that the graph has the original factor $1/(p+q)!$ which produces $(1/p!)\cdot(1/q!)$ if combined with the $C(p, q)$. Then we find that we can obtain the weight simply by *calculating the correct weight of each 2PI part separately and connecting these with the factor* $1/2!$. It is easy to generalize the above argument for the case that several kinds of vertices are contained and for higher terms on the right-hand side of Eq. (4·7) (note*) that $C(p+q+\cdots+r+s, p)\cdot C(q+\cdots+r+s, q)\cdots C(r+s, r)=(1/p!)\cdot(1/q!)\cdots(1/r!)\cdot(1/s!)$). So we associate every 2PI part in Eq. (4·7) with the factor $1/2!$ to keep the correct weight of the graphs. As mentioned in § 3.4 this kind of argument is also applicable to Eq. (3·9).

Thus we reach the following relation:

$$\left.\frac{\delta\phi_2{}^c}{\delta J_2}\right|_{\phi_1{}^c, J_3, J_4} =$$
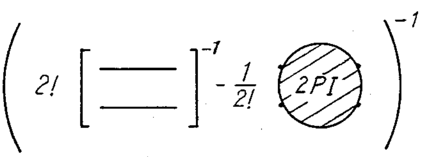
(4·8)

Then we get the 2-body BS kernel and 2-body BS equation,

$$\frac{\delta^2\Gamma_2{}^c}{\delta\phi_2{}^c\delta\phi_2{}^c}=$$
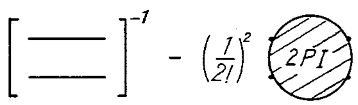
, (4·9)

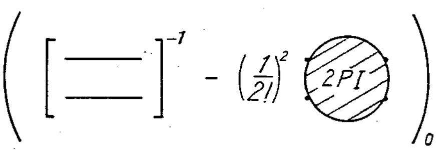
$\Delta\phi_2{}^c=0$. (4·10)

In a similar way we can proceed to the third step and get the 3-body kernel and BS equation,

$$\frac{\delta^2\Gamma_3{}^c}{\delta\phi_3{}^c\delta\phi_3{}^c}=$$
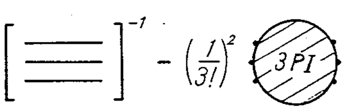
, (4·11)

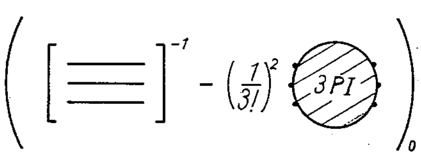
$\Delta\phi_3{}^c=0$. (4·12)

All the above results coincide with the well-known expressions (for instance, see Refs. 2) and 4)).

---

*) This property also supports the sum-up rule.

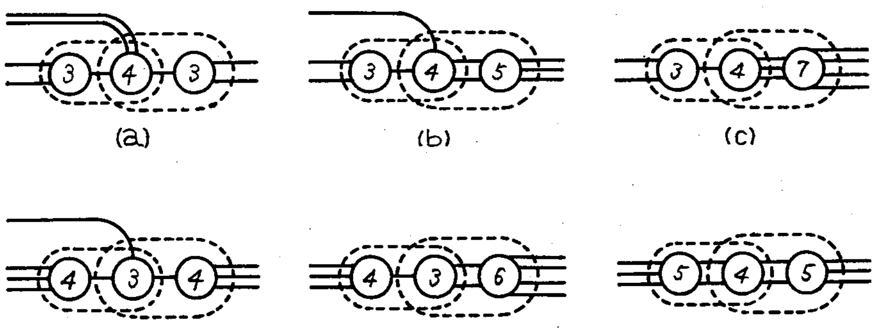

Fig. 20. The troublesome graphs: The number in each circle stands for that of lines attached to the circle.

Our method presented here helps us to elucidate the problems which have to be solved when we proceed to higher channels, or N-body case with $N \geq 5$.

Let us consider the quantity $(\delta\phi_5{}^c/\delta J_5)_{\phi_1{}^c,\cdots,\phi_4{}^c}$ to get the expression of $\delta^2\Gamma_5{}^c/\delta\phi_5{}^c\delta\phi_5{}^c$. It is assumed here that $N \geq 5$ so that $\Gamma_5{}^c = \Gamma_5{}^c[\phi_1{}^c, \cdots, \phi_4{}^c, J_5, \cdots, J_N]$ actually.

As in § 3.4 we can get the expression for $\delta\phi_5{}^c/\delta J_5$ as a functional of $\phi_1{}^c$, $\phi_2{}^c$, $\phi_3{}^c$, $\phi_4{}^{c,p}$, $J_5, \cdots, J_N$. After that we must transform J_5 to $\phi_5{}^c$. For this purpose we need similar analysis as in Appendix B. We notice that the structures shown in Figs. 20(a) ~(f) (especially (f)) cause problems similar to the one pointed out in Fig. 12 but they are more troublesome. They prevent us from defining the largest 5-legged part without ambiguity. We have to solve the combinatorial problem for these graphs in order to get the correct 5-body BS equation. This is under investigation.

Acknowledgements

The author would like to express his sincere gratitude to Professor R. Fukuda for helpful discussion and suggestions throughout the work. He is also grateful to his colleagues at Physics Department of Keio University for discussion and encouragement.

Appendix A
—— *The General Form of the N-Body BS Equation* ——

Bound states and resonances are identified with the presence of poles in the Green's functions. Here we study this fact briefly but in a general way. Then the formal N-body bound-state equation (Eq. (1·8)) is derived.

Consider the second derivative of W,

$$(N!)^2\frac{\hbar}{i}\frac{\delta^2 W}{\delta J_N\delta J_N} = \langle 0|T\varphi(x_1)\cdots\varphi(x_N)\varphi(y_1)\cdots\varphi(y_N)|0\rangle - \langle 0|T\varphi(x_1)\cdots\varphi(x_N)|0\rangle\langle 0|T\varphi(y_1)\cdots\varphi(y_N)|0\rangle\,. \tag{A·1}$$

We concentrate on extracting bound state $|P_B\rangle$ which appears in N-body channel defined by $(x_1, x_2, \cdots, x_N)$ and $(y_1, y_2, \cdots, y_N)$. It is assumed that it does not couple to channels lower than N,

$$\langle 0|\varphi(x_1)\cdots\varphi(x_N)|P_B\rangle \neq 0\,, \tag{A·2}$$

$$\langle 0|\varphi(x_1)\cdots\varphi(x_i)|P_B\rangle = 0\,, \quad (i \leq N-1) \tag{A·3}$$

where P_B stands for 4-momentum with $P_B{}^2 = m_B{}^2$. We call this state *pure N-body bound state,* where we assume that the diagonalization of the i-body channel from $i=1$ to $i=N$ has been performed.

Inserting a complete set of states into the appropriate place*) of the right-hand side of Eq. (A·1), we extract the intermediate state that corresponds to one pure N-body bound state.**) The T-product in the first term on the right-hand side of Eq. (A·1) contains $(2N)!$ terms corresponding to the order of the operators. But we concentrate on the terms in which the smallest values of the time component of $(x_1, x_2, \cdots, x_N)$ is larger than the largest value of those of $(y_1, y_2, \cdots, y_N)$. From this contribution we get

$$(N!)^2 \frac{\hbar}{i} \frac{\delta^2 W}{\delta J_N \delta J_N}$$

$$= \int d^4P\, \theta(P^0)\delta(P^2 - m_B{}^2)\langle 0|T\varphi(x_1)\cdots\varphi(x_N)|P\rangle\langle P|T\varphi(y_1)\cdots\varphi(y_N)|0\rangle\,. \tag{A·4}$$

New coordinates are introduced here,

$$X = \frac{1}{N}(x_1 + \cdots + x_N)\,; \quad Y = \frac{1}{N}(y_1 + \cdots + y_N)\,,$$

$$r_{x_j} = x_j - x_{j+1}\,; \qquad r_{y_j} = y_j - y_{j+1}\,. \quad (j=1, \cdots, N-1) \tag{A·5}$$

Then we notice that***)

$$x_j - y_k = R + f_j(r_x) - f_k(r_y)\,, \tag{A·6}$$

where $R = X - Y$ and $f_j(r_x)(f_k(r_y))$ is dependent on $r_x(r_y)$ but independent of both X and Y. Noting the relation $\varphi(x) = e^{i\hat{P}\cdot x}\varphi(0)e^{-i\hat{P}\cdot x}$ and using $\hat{P}_\mu|0\rangle = 0$ we find

$$(N!)^2 \frac{\hbar}{i}\langle 0|T\varphi(x_1)\cdots\varphi(x_N)|P\rangle\langle P|T\varphi(y_1)\cdots\varphi(y_N)|0\rangle$$

$$= \sum_{S(x';y')} \theta(R^0 + f_{N'}^0(r_x) - f_{N'}^0(r_y))\theta(r_{x_1'}^0)\cdots\theta(r_{x_{N-1}'}^0)\theta(-r_{y_{N-1}'}^0)\cdots\theta(-r_{y_1'}^0)$$

$$\times \exp\{-iP\cdot(R + f_{N'}(r_x) - f_{N'}(r_y))\}$$

$$\times \langle 0|\varphi(0)\exp(-i\hat{P}\cdot r_{x_1'})\varphi(0)\cdots\varphi(0)\exp(-i\hat{P}\cdot r_{x_{N-1}'})\varphi(0)|P\rangle$$

---

*) From Eq. (A·3) the second term on the right-hand side of Eq. (A·1) does not contribute.

**) For simplicity we assume here that this state is not degenerate, but the proof below does not change very much even if it is degenerate.

***) $r_{x_N} \equiv x_N - x_1 = -(r_{x_1} + \cdots + r_{x_N})$,
$x_1 = X + (1/N)r_{x_1} + (1/N)(r_{x_1} + r_{x_2}) + \cdots + (1/N)(r_{x_1} + \cdots + r_{x_{N-1}})$, etc.

$$\times\langle P|\varphi(0)\exp(i\hat{P}\cdot r_{y'_{N-1}})\varphi(0)\cdots\varphi(0)\exp(i\hat{P}\cdot r_{y'_1})\varphi(0)|0\rangle \tag{A·7}$$

$$\equiv -\frac{1}{2\pi i}e^{-iP\cdot R}\int dk^0\frac{e^{-ik^0\cdot R^0}}{k^0+i\varepsilon}G(r_x, r_y, k^0, P)\,. \tag{A·8}$$

Here we have employed the following notations; $R+f_{N'}(r_x)-f_{N'}(r_y)\equiv x'_N-y'_N$, superscript zero denotes the time component of the corresponding four vector, $(x'_1, \cdots, x'_N)$ or $(y'_N, \cdots, y'_1)$ is one of the permutations of $(x_1, \cdots, x_N)$ or $(y_1, \cdots, y_N)$ respectively, and $\sum_{S(x';y')}$ means the summation over all these possible permutations.

Taking into account the contribution from the terms in the T-product where one of the permutations of $(\phi(x_1), \phi(x_2), \cdots, \phi(x_N))$ comes after that of $(\phi(y_1), \phi(y_2), \cdots, \phi(y_N))$ (the opposite case of Eq. (A·4)), the Fourier transform of the quantity in question takes the form

$$(N!)^2\frac{\hbar}{i}\frac{1}{(2\pi)^4}\int d^4R\; e^{iQ\cdot R}\frac{\delta^2 W}{\delta J_N\delta J_N}$$
$$=-\frac{1}{4\pi i\sqrt{\boldsymbol{Q}^2+m_B{}^2}}\left(\frac{g(r_x, Q_B{}^+)\bar{g}(r_y, Q_B{}^+)}{Q^0-\sqrt{\boldsymbol{Q}^2+m_B{}^2}+i\varepsilon}-\frac{g(r_y, Q_B{}^-)\bar{g}(r_x, Q_B{}^-)}{Q^0+\sqrt{\boldsymbol{Q}^2+m_B{}^2}-i\varepsilon}\right), \tag{A·9}$$

where $Q_B{}^{\pm}=(\sqrt{\boldsymbol{Q}^2+m_B{}^2}, \pm\boldsymbol{Q})$. Thus the pure N-body bound state constituting of $\varphi(x_1)\cdots\varphi(x_N)$ is completely extracted as a pole of the total energy of N-body channel. The other terms in the T-product of Eq. (A·1) do not contribute to the channel defined by $(x_1, x_2, \cdots, x_N)$ and $(y_1, y_2, \cdots, y_N)$.

Using Eqs. (1·3) and (1·5), we get

$$-i!k!\frac{\delta^2 W}{\delta J_i\delta J_k}\frac{\delta^2\Gamma_N}{\delta\phi_k\delta\phi_j}=\delta_{i,j}\,, \tag{A·10}$$

where space-time coordinates and integration over those variables are suppressed. Then it is easily derived that

$$-N!\left[\sum_{j,k}^{N-1}\frac{\delta^2 W}{\delta J_N(x)\delta J_j(z)}j!\frac{\delta^2\Gamma_{N-1}}{\delta\phi_j(z)\delta\phi_k(w)}k!\frac{\delta^2 W}{\delta J_k(w)\delta J_N(y')}+\frac{\delta^2 W}{\delta J_N(x)\delta J_N(y')}\right]N!$$
$$\times\frac{\delta^2\Gamma_N}{\delta\phi_N(y')\delta\phi_N(y)}=I_N(x, y)\,, \tag{A·11}$$

where

$$I_N(x, y)=\frac{1}{N!}\sum_S\delta(x_1-y'_1)\cdots\delta(x_N-y'_N)\,. \tag{A·12}$$

In the above expression $(y'_1, \cdots, y'_N)$ stands for one of the permutations of $(y_1, \cdots, y_N)$ and $\sum_S$ implies summation over all possible $(y'_1, \cdots, y'_N)$. The Fourier transform can be written in the following form,

$$\int dq'[F^Q(q, q')+W^Q_{N,N}(q, q')]\Gamma^Q_{N,N}(q', p)=I(q, p)\,. \tag{A·13}$$

Here Q, q and p are momenta corresponding to $R=X-Y$, r_x and r_y respectively (there are $(N-1)$ q's and p's). $F^Q(q, q')$ denotes the Fourier transform of the first term in the square bracket on the left-hand side of Eq. (A·11). The other notations will be clear. Note that the momentum Q is not integrated and the right-hand side is independent of Q.

Observing that $W_{N,N}^{Q}$ has poles corresponding to pure N-body bound states while $F^{Q}(q, q')$ does not, we realize the following theorem.

THEOREM 2 *The pure N-body bound-state energy appears as a zero of the second derivative by ϕ_N of the Nth-effective action.*

Inserting the vacuum solution $\varphi_i^{(0)}$ the N-body BS equation therefore becomes

$$(\Gamma_{N,N}^{Q}(q, p))_0 \Delta\phi(p)=0 \qquad (\mathrm{A}\cdot 14)$$

or Eq. (1·8) in the coordinate representation. All the possible bound states will be found if one solves Eq. (1·8) successively starting from the case $N=1$. This is the case even if the channel diagonalization is not performed; we have only to look for new bound state which has not appeared in the lower channels.

Appendix B

—— *General Structures of Figs. 9 and 11* ——

Let us go back to Fig. 9. If we take a 3-legged part which partially contains B-part, general structure of this graph can be expressed as Fig. 21. The closed broken line C in Fig. 21(b) is assumed to be such a 3-legged part which has b-part in common with B-part. Adopting the notation in which $\alpha, \beta, \cdots, \zeta$ stand for the number

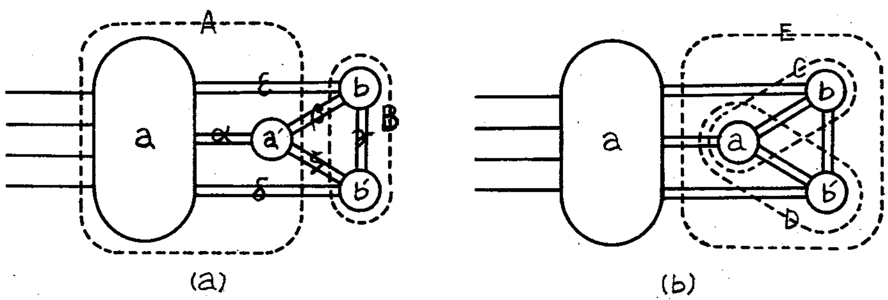

Fig. 21. The general structure of Figs. 9 and 11: The parts $\alpha, \beta, \cdots, \zeta$ stands for bundles of lines connecting between a- and a'-parts, a'- and b-parts, $\cdots$, a'- and b'-parts respectively.

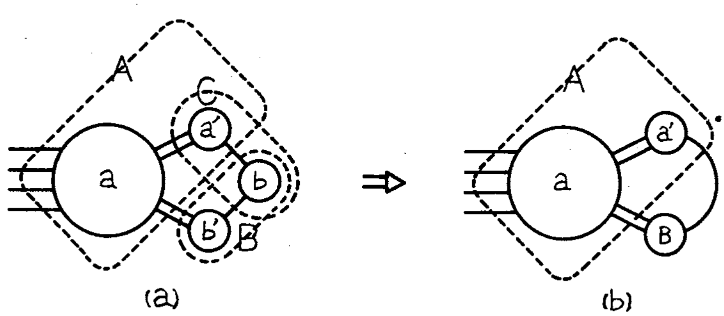

Fig. 22. $(\alpha, \beta, \gamma, \delta, \varepsilon, \zeta)=(2, 1, 1, 2, 0, 0)$.

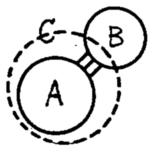

Fig. 23. Example of the graph for which we cannot establish the statement.

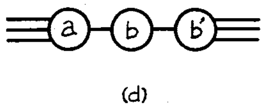

Fig. 24. The troublesome cases.

of lines contained in $\alpha, \beta, \cdots, \zeta$-parts respectively, we get $\alpha+\zeta+\gamma+\varepsilon=3$(C-part), $\varepsilon+\beta+\zeta+\delta=3$ (B-part). The assumption mentioned in § 3.3 remains true if E-part in Fig. 21 is a 3-legged part ($\varepsilon+\alpha+\delta=3$). Note that the graph is constructed with $\phi_1{}^c$, $\phi_2{}^c$ so that the cases with $\varepsilon+\alpha+\delta=1, 2$ are excluded. Therefore we have to study only the case $\varepsilon+\alpha+\delta\geq 4$.

Considering again the fact that the graph is built with $\phi_1{}^c$, $\phi_2{}^c$, it follows that $\alpha+\delta+\gamma+\beta\geq 3$ (D-part).

The connectivity of each part requires $\alpha\geq 1$ (A-part), $\gamma\geq 1$(B-part), $\beta\geq 1$ (C-part). Then the only allowed set of $(\alpha, \beta, \cdots, \zeta)$ is*)

$$(\alpha, \beta, \gamma, \delta, \varepsilon, \zeta)=(2, 1, 1, 2, 0, 0)\,, \tag{B·1}$$

which corresponds Fig. 22(a). But the graph should be made up of $\phi_2{}^c$, so the closed broken line C or Case Eq. (B·1) does not actually exist**) ending up with Fig. 22(b).

In fact there are other cases which should be considered. These are the cases where the broken line C intersects external lines. But the above arguments are valid for such cases as well. So the statement in § 3.3 is proved.

In the above discussion the crucial point is that the A-part has external lines. Otherwise, we have to consider the case like Fig. 23 where the above conditions for C-part break down.

Next we come back to Fig. 11 and follow the discussion similar to the above one. Then the following cases seem to prevent us from defining the larger 4-legged part.

$$\begin{aligned}(\alpha, \beta, \gamma, \delta, \varepsilon, \zeta)=&(2, 1, 2, 3, 0, 0) \quad (a)\,,\\ &(3, 2, 1, 2, 0, 0) \quad (b)\,,\\ &(2, 1, 1, 2, 1, 0) \quad (c)\,,\\ &(3, 1, 1, 3, 0, 0) \quad (d)\,.\end{aligned} \tag{B·2}$$

Cases (a), (b), (c) are shown in Fig. 12 and (d) in Fig. 24. But Fig. 24 causes no problem like the case of Fig. 22 since the graph is built with $\phi_2{}^c$, but (a) (b) and (c) are the origin of the problem as mentioned before.

*) This result is easily obtained by a personal computer.

**) Of course, we could set more strict constraint from the beginning so that Eq. (B·1) cannot be allowed.

Appendix C

—— *Proof of the Theorem 1; D_4 Simple Net=[D_4 Chain]$^{-1}$* ——

The D_4 chain is clearly defined as*)

$$D_4\ \text{chain}=-\frac{1}{4!}I_4\{I_0^{-1}-I_0^{-1}KI_0^{-1}\}\,, \tag{C·1}$$

$$I_0(x;y)=\phi_2{}^c(x_1,y_1)\phi_2{}^c(x_2,y_2)\phi_2{}^c(x_3,y_3)\phi_2{}^c(x_4,y_4)\,, \tag{C·2}$$

$$K=\sum_{i=1}^{\infty}(-1)^{i-1}K_i\,, \tag{C·3}$$

$$K_i=\sum_{j=0}^{m_i}K_j^{i-j}\,, \tag{C·4}$$

$K_m{}^l=$ [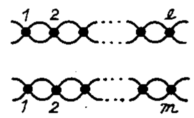] . (C·5)

In Eq. (C4), $m_i=i/2$ or $(2i+1)/2$ depending on whether i=even or odd. We need further explanation of Eq. (C·5).**) First, black dot on the right-hand side stands for D_4 (as in all the graphs in this appendix), that is,

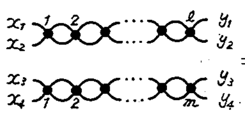

$$=[\phi_2{}^c(x_1,z_1)\phi_2{}^c(x_2,z_2)]^{1/2}\left(\frac{1}{2}\overline{D_4}\right)^l_{z_1,z_2;w_1,w_2}[\phi_2{}^c(w_1,y_1)\phi_2{}^c(w_2,y_2)]^{1/2}$$

$$\times[\phi_2{}^c(x_3,z_3)\phi_2{}^c(x_4,z_4)]^{1/2}\left(\frac{1}{2}\overline{D_4}\right)^m_{z_3,z_4;w_3,w_4}[\phi_2{}^c(w_3,y_3)\phi_2{}^c(w_4,y_4)]^{1/2}\,, \tag{C·6}$$

where we have employed, along with any function $X(x_1,x_2,x_3,x_4)$, the function

$$\overline{X}(x_1,x_2,x_3,x_4)$$
$$=X(y_1,y_2,y_3,y_4)[\phi_2{}^c(y_1,x_1)]^{1/2}[\phi_2{}^c(y_2,x_2)]^{1/2}[\phi_2{}^c(y_3,x_3)]^{1/2}[\phi_2{}^c(y_4,x_4)]^{1/2}\,. \tag{C·7}$$

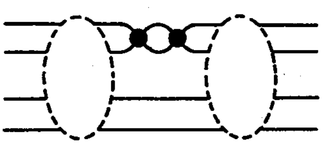

Fig. 25. The structure of the graphs that give vanishing contribution to Eq.(C·8): Two closed broken-lines stand for any 8-*legged part*.

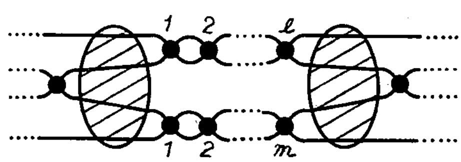

Fig. 26. The non-simple-type graph.

*) This is also defined by the second derivative of the following quantity by $\phi_4{}^c$ fixing $\phi_1{}^c$, $\phi_2{}^c$ and $\phi_3{}^c$; $(1/2)\mathrm{tr}\{\ln[1+(1/2)\overline{D_4}]-(1/2)\overline{D_4}-(1/2)[(1/2)\overline{D_4}]^2-(1/4!)[\overline{\phi_4{}^{c,p}}]^2\}$.

**) I_4 is already defined in Eq. (A·12).

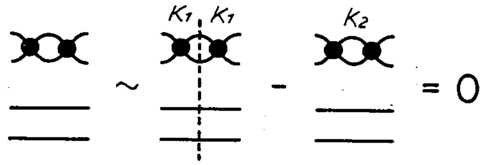

Fig. 27. Mechanism of cancellation: The first (second) term on the right-hand side stands for the contribution to the graph on the left-hand side from the term $K_1\tilde{I}_0^{-1}K_1(K_2)$ in $K\tilde{I}_0^{-1}K(K)$.

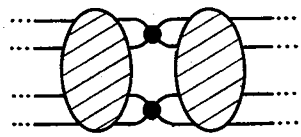

Fig. 28. The possible structure for the simple-type graph: The shaded part represents the intertwined part.

As always appearing squared, the square roots cause no ambiguity. Second, [⋯] implies that $K_m{}^l$ represents 6 different types if $l \neq m$ and 3 types if $l=m$.

Now we study the inverse of Eq. (C·1) which can be written as

$$(D_4 \text{ chain})^{-1} = -4!I_4(I_0+K+KI_0^{-1}K+KI_0^{-1}KI_0^{-1}K+\cdots)\,. \tag{C·8}$$

Our aim is to prove that this coincides with D_4 simple net. The proof is divided into two steps. First we will show that terms which can be viewed as having the stucture of Fig. 25(non-simple-type) vanish in Eq. (C·8). And then it is proved that the remaining type (simple-type) of graphs corresponds to simple net with right weight.

A given non-simple-type graph may be one element of $K_m{}^l$, otherwise it has necessarily the structure of Fig. 26 ($l \geq 2$, $m \geq 0$). We call the shaded parts in Fig. 26 *intertwined parts* where two adjacent D_4 vertices are connected by one and only one line. Noting that the graphs of K do not have intertwined parts in itself, intertwined parts surely come from I_0^{-1} in Eq. (C·8). So we have only to prove that the graphs on the left-hand side of Eq. (C·6) vanish in Eq. (C·8). For $l=2$, $m=0$ the graph is generated by the terms K and $KI_0^{-1}K$ in Eq. (C·8), so it is cancelled out (Fig. 27). By the same analysis we see that the graphs with $l \geq 2$, $m=0$ are cancelled as well. For the case where $l \geq 2$, $m \geq 1$ we make use of mathematical induction as follows (see Eq. (C·9) below). All cases are exhausted if we consider the cases where the upper leftest D_4 vertex comes from $K_1, K_2, \cdots$, or K_{l+m}. By the assumption about lower hierarchy only the four underlined terms in Eq. (C·9) remain. But these four terms are also cancelled out as illustrated in Eq. (C·9).

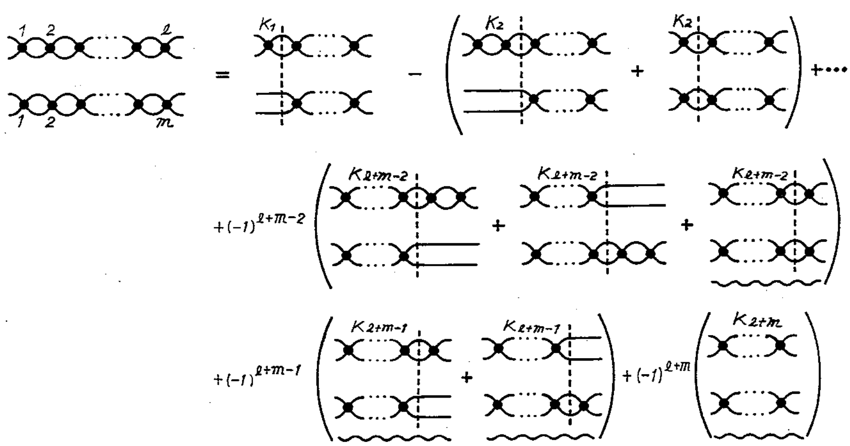

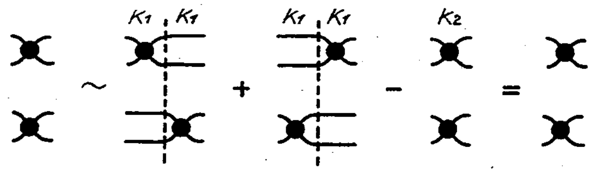

Fig. 29. The generation of the subpart illustrated in Fig. 28.

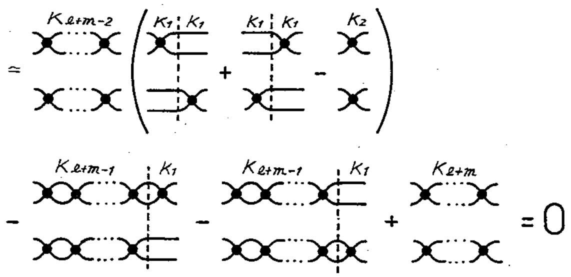

(C·9)

Thus Eq. (C·8) is able to be rewritten as

$$(D_4 \text{ chain})^{-1} = -4!I_4(I_0 + K' + K'\tilde{I}_0^{-1}K' + K'\tilde{I}_0^{-1}K'\tilde{I}_0^{-1}K' + \cdots)\,, \qquad (\text{C}\cdot 10)$$

where $K' = K_0^1 - K_1^1$ and $\tilde{I}_0^{-1}$ implies that the adjacent two D_4 vertices in K' which are attached to both sides of $\tilde{I}_0^{-1}$ are directly connected by one and only one line so that all the graphs in Eq. (C·10) may become simple-type. Note that each $\tilde{I}_0^{-1}$ thus corresponds to intertwined part.

If a simple-type graph does not have the structure of Fig. 28 it appears with right weight, because there is only one way we generate it in Eq. (C·10). Note that each intertwined part comes form $\tilde{I}_0^{-1}$. In other cases, however, it is also proved that it appears with right weight by noting that the subpart shown in Fig. 28 is generated as Fig. 29 and by using the induction with respect to the number of the subparts shown in Fig. 28. So Theorem 1 holds.

References

1) Y. Nambu, Prog. Theor. Phys. **5** (1950), 614.
E. E. Salpeter and H. A. Bethe, Phys. Rev. **84** (1951), 1232.
2) N. Nakanishi, Prog. Theor. Phys. Suppl. No. 43 (1969); Prog. Theor. Phys. Suppl. No. 95 (1988), ed. N. Nakanishi.
3) S. Machida and H. Nakkagawa, Prog. Theor. Phys. **54** (1975), 243, 510.
K. Tesima, Prog. Theor. Phys. Suppl. No. 77 (1983), 285.
4) M. Komachiya, M. Ukita and R. Fukuda, Phys. Rev. **D40** (1990), 2654.
5) J. Glimm and A. Jaffe, *Lecture Notes in Physics* (Springer, Berlin, 1975), **39**, p. 118.
6) M. Combescure and F. Dunlop, Ann. of Phys. **122** (1979), 102.
7) A. Cooper, J. Feldman and L. Rosen, Ann. of Phys. **137** (1981), 146, 213; J. Math. Phys. **23** (1982), 846; Phys. Rev. **D25** (1982), 1565.
8) Y. Yokojima, M. Komachiya and R. Fukuda, Keio Univ. Preprint (1991).
9) R. Fukuda, Prog. Theor. Phys. **78** (1987), 1487.
10) C. De Dominicis and P. C. Martin, J. Math. Phys. **5** (1964), 14, 31.
11) A. N. Vasil'ev and A. K. Kazanskii, Theor. Math. Phys. **12** (1972), 875; **14** (1973), 215.
Yu. M. Pis'mak, Theor. Math. Phys. **18** (1974), 211.
A. N. Vasil'ev, A. K. Kazanskii and M. Pis'mak, Theor. Math. Phys. **19** (1974), 443; **20** (1974), 754.
12) T. Spencer, Commun. Math. Phys. **44** (1975), 144.
13) G. Jona-Lasinio, Nuovo Cim. **34** (1964), 1790.

14) For example,
S. Coleman and E. Weinberg, Phys. Rev. **D7** (1973), 1888.
R. Jackiw, Phys. Rev. **D9** (1974), 1686.
John M. Cornwall, R. Jackiw and E. Tomboulis, Phys. Rev. **D10** (1974), 2428.
D. J. Gross and A. Noveu, Phys. Rev. **D10** (1974), 3235.
15) R. Fukuda, M. Komachiya and M. Ukita, Phys. Rev. **D38** (1988), 3747.
16) M. Komachiya, M. Ukita and R. Fukuda, Phys. Rev. **D42** (1990), 2792.